

Accounts

Ultrafast Energy Transfer Dynamics at Solid/Liquid Interfaces as Investigated by Photothermal Spectroscopy

Isao Tsuyumoto and Tsuguo Sawada^{*,†}

Department of Environmental Systems Engineering, Kanazawa Institute of Technology,
7-1 Ohgigaoka, Nonoichi, Ishikawa 921-8501

[†]Department of Applied Chemistry, School of Engineering, The University of Tokyo, 7-3-1 Hongo, Tokyo 113-8656

(Received October 1, 1999)

Recent studies on ultrafast energy transfer at solid/liquid interfaces were reviewed, focusing on our developed photothermal techniques: femtosecond transient reflectivity (fs-TR) method, femtosecond transient reflecting grating (fs-TRG) method, and picosecond surface plasmon resonance transient reflecting grating (ps-SPR-TRG) method. Firstly, Pt/aqueous electrolyte interfaces were measured using the fs-TR method. An ultrafast relaxation component of 20 fs was first observed in the Pt/HCl (aq) and Pt/H₂SO₄ (aq) interfaces, in which the anions (Cl[−] and SO₄^{2−}) have strong affinity to the Pt surface. It was suggested that this is due to the scattering of non-thermalized electrons by adsorbed anions. Secondly, TiO₂/KSCN (aq) interfaces were measured using the fs-TRG method. Ultrafast relaxation components (110—690 fs) were observed in the TRG signals. This marked the first observation of the contribution of nonequilibrium holes to the energy transfer at TiO₂/KSCN (aq) interfaces. Thirdly, Au/NaCl (aq) interfaces were measured using ps-SPR-TRG method, focusing at both the behavior of hot electrons and thermal diffusion. The results indicated that an ultrafast energy transfer process occurs prior to the heat diffusion and this process is hindered by the adsorbed ions.

The elementary processes of solid/liquid interface reactions represent a very exciting and important area of science and technology. Especially, the energy transfer dynamics at solid/liquid interfaces plays a crucial role in various processes such as electrode reaction, photocatalysis, photosynthesis, and corrosion.^{1–5} Understanding of the ultrafast charge transfer dynamics at the interface is fundamentally important for designing functional electrode surfaces and for controlling the interfacial reactions. The contribution of hot electrons in photo-excited reaction has attracted much attention because the initial reaction proceeds in ultrafast time region when the photo-excited electrons are not in equilibrium with other electrons. Hot electrons mean the photo-excited electrons that are not in equilibrium with other electrons. However, monitoring of the hot electrons at solid/liquid interfaces accompanies experimental difficulties because of their buried nature. Actually many investigations on solid surfaces have been performed using various methods such as laser spectroscopy, AES, UPS, XPS, whereas few methodologies have been reported on ultrafast dynamics at solid/liquid interfaces.^{6–13}

Photothermal spectroscopy is one of the most useful methods that allow in situ measurements with high time-resolution, high sensitivity, and high interfacial selectivity.^{14,15} This

method utilizes nonradiative relaxation processes of electrons while fluorescence (luminescence) spectroscopy utilizes radiative relaxation processes. It is applicable to unmodified interfaces because it does not require luminescence or fluorescence.

Our aim is to investigate the ultrafast dynamics at solid/liquid interfaces by using photothermal spectroscopy. Development of spectroscopic methodologies appropriate for the solid/liquid interfaces are indispensable for the measurements. We have developed high time-resolved photothermal techniques: femtosecond transient reflectivity (TR) method, femtosecond transient reflecting grating (TRG) method, and picosecond surface plasmon resonance (SPR) TRG method. We have applied these methods to solid surfaces and solid/liquid interfaces, and successfully obtained significant information on photoexcited carriers.^{16–28}

In this review, we summarize our recent studies on ultrafast dynamics at solid/liquid interfaces using our developed photothermal techniques, not over the entire broad range of photothermal spectroscopy.

1. Observation of Ultrafast Relaxation Process at Pt/Electrolyte Interfaces by Femtosecond Transient Reflectivity (TR) Method

Firstly, transient reflectivity measurement was performed in order to obtain information of ultrafast dynamics at solid/liquid interfaces. Transient reflectivity (TR) method simply monitors transient reflectivity change induced by a pump beam using a probe beam.¹⁶ When a sample surface is irradiated by the pump beam, electronic excitation occurs in the irradiated spot. The excitation brings about refractive index change, i. e., reflectivity change. Therefore information on electronic excitation can be obtained by monitoring the intensity of the reflected light of the probe beam. By using a femtosecond pulsed laser with an autocorrelation of 170 fs, the method was successfully extended to 10 femtosecond time region. Details on experimental setup have been described in our previous review.²⁹

Hibara et al. measured TR for a polycrystalline Pt thin-film with thickness of 30 nm immersed in aqueous electrolyte solutions, focusing the interfacial electronic interaction between Pt and anions (Fig. 1).¹⁶ By using the thin-film instead of bulk Pt, the diffusion of hot electrons perpendicular to the interface could be prevented. Three types of aqueous electrolyte solutions were used for the measurement: 0.1 mol dm⁻³ HClO₄, 0.1 mol dm⁻³ H₂SO₄ and 0.1 mol dm⁻³ HCl. Since the affinities of Cl⁻ and SO₄²⁻ are stronger than ClO₄⁻, the effect of affinity to the ultrafast dynamics could be investigated.

Figure 2 shows TR responses at the Pt/electrolyte solution interfaces. The ratio of reflectivity change ($\delta R/R$) is on the order of 10⁻⁵ to 10⁻⁴. The curves in Fig. 2 correspond to the following processes. Electrons within the optical penetration depth (less than 15 nm) are excited, and subsequently the excited electrons are thermalized within 1 ps. The reflectivity change within 1 ps correspond to an energy transfer process from the electrons to the Pt lattice by way of electron-phonon coupling, and that after thermalization corresponds to electron temperature.

The analysis of the curves was performed considering instrumental functions. It was found the bi-exponential model was only valid for the TR responses for pure water and HClO₄. The TR responses for HCl and H₂SO₄ were suitably fitted with tri-exponential model. The fitting parameters are summarized in Table 1. The first and second components correspond to the electron-phonon coupling relaxation and heat diffusion, respectively. The relaxation times

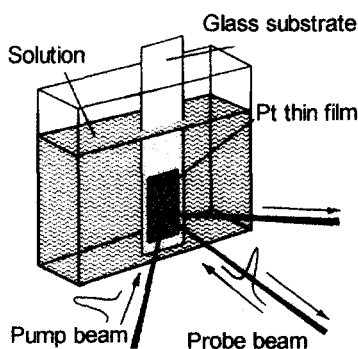


Fig. 1. Schematic illustration of the experimental arrangement around the sample cell for femtosecond time-resolved transient reflectivity measurements. The Pt thin film was 30 nm thick, and aqueous solutions used were 0.1 M HClO₄, 0.1 M HCl, 0.1 M H₂SO₄, and pure water.

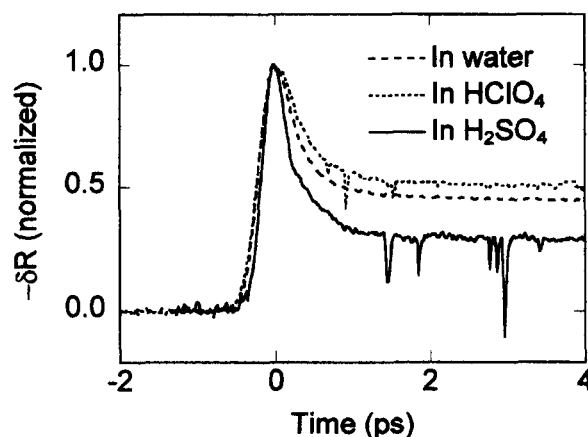


Fig. 2. Transient reflectivity responses at the Pt/aqueous electrolyte solutions interfaces.

Table 1. Time Constants and Pre-exponential Factors Calculated as Fitting Parameters for the Transient Reflectivity Responses from Pt/Aqueous Electrolyte Solutions Interfaces

	τ_1 (ps)	τ_2 (ps)	τ_3 (ps)	C_1	C_2	C_3
Pure water	0.3	60		0.72	0.28	
HClO ₄	0.4	100		0.66	0.34	
HCl	0.6	100	0.02	0.03	0.02	0.95
H ₂ SO ₄	0.7	100	0.02	0.03	0.02	0.95

of electron-phonon coupling agree with those reported in an early work of the Pt surface in the UHV.³⁰ On the other hand, the third component (20 fs) in HCl and H₂SO₄ was first observed in this study. The relaxation time 20 fs is much faster than the processes of electron-phonon coupling, and mechanisms faster than the electron-phonon coupling should be considered. It is natural to consider that this component reflects the strong affinity of the anions to the Pt surface. It is proposed that the third component is due to non-radiative relaxation of non-thermalized electrons (NTEs) through interfacial scattering by adsorbed anions. The NTEs are the electrons which are not in equilibrium with other electrons below the Fermi level, i. e., do not follow the Fermi distribution. The NTEs are first excited by incident photons, and they scatter with other electrons to attain the Fermi distribution. It is considered that this process is affected by the adsorbed anion and appeared as the third process.

In summary, the Pt/electrolyte interfaces were measured using the femtosecond TR method. A novel ultrafast relaxation component (20 fs) was found in the Pt/HCl (aq) and Pt/H₂SO₄ (aq) interfaces. It was proposed that this is due to the scattering of non-thermalized electrons by adsorbed anions.

2. Femtosecond Transient Reflecting Grating (TRG) Method and Its Application to Monitoring of Ultrafast Energy Transfer at TiO₂/KSCN (aq) Interfaces

As mentioned above, the TR method monitors extremely small reflectivity changes ($\delta R/R = 10^{-5}$ – 10^{-4}). This causes low S/N ratio of the TR signals and experimental difficulties in measurements. In order to improve S/N ratio of the ultrafast signals, Morishita et al. developed a femtosecond transient reflecting grating (TRG) method and successfully applied it to solid/liquid interfaces.^{20,24}

The principle of the transient reflecting grating (TRG) method is

shown in Fig. 3. Two pump pulses of the same wavelength λ_{pump} cross on a sample surface, to form an optical interference pattern with a fringe spacing Λ , $\Lambda = \lambda_{\text{pump}}/2\sin\theta$ where θ is a pump beam incident angle normal to the surface. This interference pattern transforms into a periodical refractive index change, which acts as a transient diffraction grating. A probe pulse is incident normal to the grating, and a diffracted light is observed. The intensity of the diffracted light is monitored as a function of the delay time of the probe beam. The TRG signal reflects dynamic information on surfaces such as refractive index change by electronic excitation and heat generation.

The experimental setup for the TRG method is shown in Fig. 4. The light source was a regeneratively amplified Ti:Sapphire laser system which had an auto-correlation of 150 fs, wavelength of 800 nm and repetition rate of 1 kHz. The output beam of the 800 nm wavelength was partly reflected by a half mirror to generate a probe beam passing through a computer controlled optical delay line. The residual beam was frequency-doubled by a BBO crystal to generate a 400 nm beam which was split into two parts. Each pump pulse had a spot size of 600 μm and the fluency was changed from 2.16 to 4.57 mJ cm^{-2} . The pump pulse had p-polarization. We wanted to study how the photo-excited carrier density affects the interface reaction. The fringe spacing was set to 2.1 μm by setting the incident angle to 5°. Polarizations of the pump and probe beams

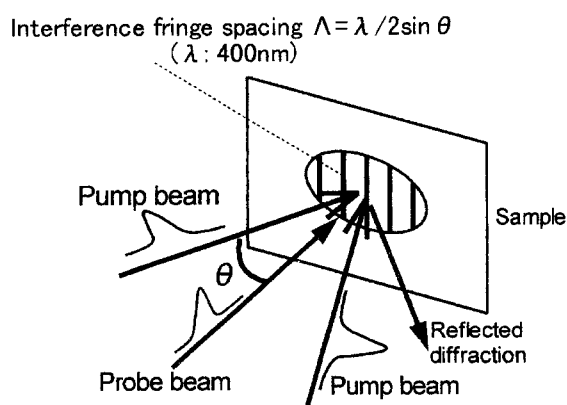


Fig. 3. Schematic illustration of the principle of the TRG method. Two pump laser pulses excite an interference fringe at the intersection, which acts as a transient reflecting grating for a probe beam.

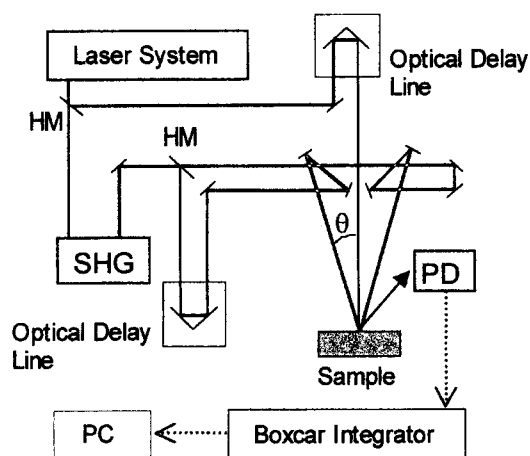


Fig. 4. Experimental setup for the femtosecond TRG method. HM, half mirror; PD, photodiode.

were perpendicular to each other. The diffracted light was detected by a PIN photodiode. The output of the photodiode was fed into a fast-gated-integrator and its average signal was recorded as a TRG response.

A sample cell was fabricated for solid/liquid interface measurements. Its optical window was made of quartz glass with optically flat surfaces and the thickness of the liquid phase could be controlled by changing the spacers. Controlling the thickness of the liquid phase was indispensable to improvement of the S/N ratio because fluctuation of the liquid phase greatly disturbs the measurement. A solid/liquid interface was prepared by pouring a KSCN (aq) solution into the sample cell. A TiO_2 single crystal was attached to the sample cell. The TiO_2 single crystal with Rutile structure (001) surfaces was purchased (K & R Creation Co., Inc.) and used without any modification. KSCN was also purchased (Wako Chemical Co., Inc.; special grade; 99.5% purity) and used without further purification. The concentrations of KSCN (aq) solution were in the range of 0–20 mM with the pump beam fluency of 4.5 mJ cm^{-2} . We intended to study how the population of adsorbate on TiO_2 affects the behavior of photo-excited carriers.

TRG responses from the interfaces between TiO_2 and KSCN (aq) in the range of 0–20 mM are shown in Fig. 5. The S/N ratio of the TRG signals was improved by decreasing the thickness of the liquid phase which prevented its fluctuation. The intensity of the TRG signals was almost the same, regardless of the thickness of the liquid phase. This indicates that the TRG signals were not from the bulk solutions but from the interface.

An increase in the TRG signal corresponds to the change in the refractive index of the sample surfaces induced by the generation of photoexcited carriers. In Fig. 5, the small fall after the peak clearly becomes greater with increasing SCN^- concentration and the small fall is never observed at the $\text{TiO}_2/\text{H}_2\text{O}$ interface. The time constants of this decay component is summarized in Table 2. The adsorption of SCN^- ion is not saturated in this concentration region, and the number of adsorbate increases with increasing concentration of SCN^- . Therefore, the increase in the intensity of the small fall reflects the phenomena involving the adsorbate (SCN^-). The maximum height of the TRG signal is almost constant in all experiments, which suggests that there is no change in the density

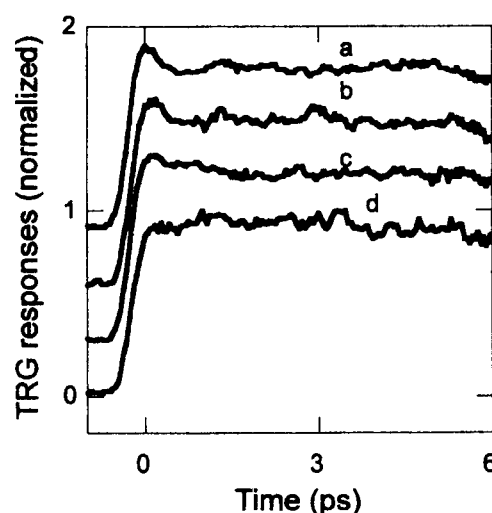


Fig. 5. Typical TRG signals from $\text{TiO}_2/\text{SCN}^-$ aq interfaces with various SCN^- concentrations. The concentrations of SCN^- are a: 20 mM, b: 15 mM, c: 10 mM, and d: 0 mM. For clarity, the signals are vertically displaced.

Table 2. Time Constants and Pre-exponential Factors Calculated as Fitting Parameters for the TRG Signals from TiO_2/KSCN (aq) Interfaces
Concentration of KSCN is fixed at 15 mM.

Pump power intensity (mW)	τ_1 (fs)	τ_2 (ps)	C_1	C_2
4	110	173	0.54	0.46
5	200	137	0.38	0.62
7	450	130	0.22	0.78
8	690	150	0.17	0.83

of pump beam fluency due to self-focusing induced by the SCN^- (aq). These facts indicate that an ultrafast relaxation process of the photoexcited holes (110–690 fs) occurs at the $\text{TiO}_2/\text{SCN}^-$ (aq) interfaces.

Figure 6 shows the intensity of the ultrafast decay component vs the concentration of SCN^- . The intensity of the ultrafast decay component increases with the increase of the SCN^- concentration; that is, the ultrafast relaxation of the photoexcited holes becomes dominant with the increase in the number of adsorbed SCN^- ions. Thus, we can presume that the observed ultrafast decay is mainly due to ultrafast hole transfer at the interfaces 110–690 fs.

Next, the photoexcited hole dynamics at several pump beam powers was considered. Figure 7 shows the dependence of the TRG responses from the $\text{TiO}_2/\text{SCN}^-$ interfaces on the number of the photoexcited carriers. The concentration of the SCN^- (aq) is all 15 mM in this experiment. Since the atomic density of the TiO_2 is 100 times higher than that of the photoexcited carriers, the absorption of the solid sample is not saturated even at high power. The intensity of the TRG signals and the relative number of the photoexcited carriers which contribute to the interfacial reaction vs. the pump beam power is plotted in Fig. 8. The intensity of the TRG signals and the relative number of the photoexcited carriers increase with the increase of the pump beam power. However, the coefficients of the increase are not as expected. This means that the ratio of the ultrafast charge transfer decreases with an increasing number of photoexcited carriers. This is probably because the path for the ultrafast charge transfer is controlled by not only the density of photoexcited carriers but also other factors, such as the number of adsorbate molecules and the number of lattice defects at the

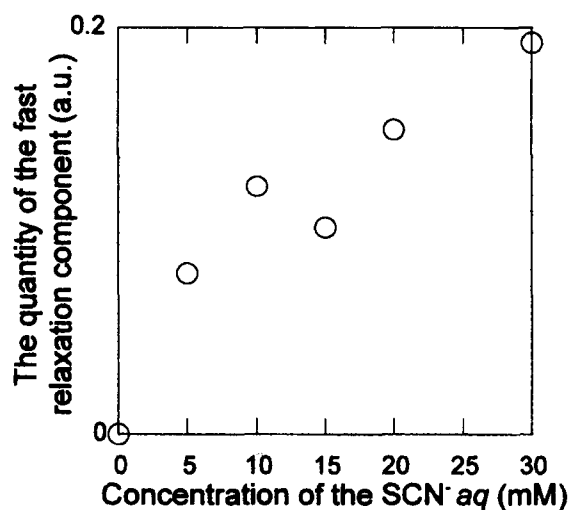


Fig. 6. Intensity of the ultrafast decay component vs. the concentration of SCN^- . The intensity of the component increases with increasing concentration of SCN^- .

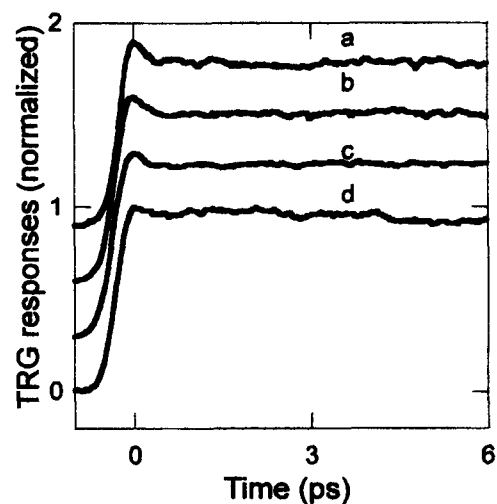


Fig. 7. Typical TRG signals from the $\text{TiO}_2/\text{SCN}^-$ aq interfaces with various pump beam powers. The intensities of the pump beam power are a: 4 mW, b: 5 mW, c: 7 mW, d: 8 mW. For clarity, the signals are vertically displaced.

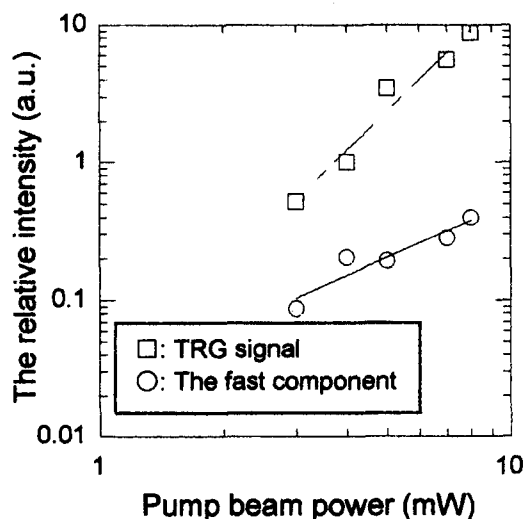


Fig. 8. Intensity of the TRG signals and the relative intensity of the fast relaxation component vs. pump beam power.

interface.

The obtained TRG signals are fitted with a double exponential decay using a least-squares method. The signals are deconvolved using an instrumental function with fwhm of 250 fs. As shown in Table 2, the time constant increases with increasing the pump beam power (110–690 fs), whereas the intensity decreases with increasing the pump beam power. The increase in the time constants is probably due to the change in path for the ultrafast charge transfer as discussed above.

Photoexcited holes exist as non-equilibrium holes on a time scale of 100 fs after which they undergo an energy dissipation process via the carrier-carrier scattering. Our experimental results suggest a role for non-equilibrium holes in the reaction at the $\text{TiO}_2/\text{SCN}^-$ interfaces. With the increase in the number of photoexcited carriers, the energy dissipation process becomes dominant and the interfacial reactive process occurs less, because the rate of the carrier-carrier scattering process increases, and vice versa. We believe this is the first observation of the contribution of nonequilibrium holes to the

reaction at $\text{TiO}_2/\text{SCN}^-$ interfaces. It is very exciting to note that the ultrafast nonequilibrium hole transfer in 110–690 fs was observed here, because it has been thought that nonequilibrium hole transfer does not occur and only equilibrated holes can be transferred across an interface. This work indicates that the nonequilibrium holes should be taken into account in interface reactions. We believe this result will provide valuable knowledge for designing electrode surfaces and controlling interfacial reactions.

3. Picosecond Transient Reflecting Grating Method under Surface Plasmon Resonance (SPR-TRG) and Its Application to Monitoring of Energy Transfer at Au/NaCl (aq) Interfaces

Femtosecond TR and TRG studies were performed to reveal ultrafast energy transfer processes at solid/liquid interfaces, focusing on the behavior of hot carriers (electrons and holes). In addition to such studies, it is highly desirable to observe all the energy transfer processes including conventional heat transfer processes in extensive time regions. In order to achieve this, picosecond transient reflecting grating method under surface plasmon resonance (SPR-TRG) has been developed.^{25–28} This method can monitor both electronic interaction and thermal energy transfer on an extensive time scale from picosecond to nanosecond. The conventional picosecond TRG method monitors only heat generation via the induced surface elastic waves.¹⁴ By applying the surface plasmon resonance condition to the TRG method, the signals of hot electrons were successfully enhanced and could be detected with a 100-times larger intensity. The SPR-TRG method allows to directly measure both ultrafast electronic interactions on a time scale of picosecond and thermal energy transfer on a time scale of nanosecond. The aim of this study is to reveal the energy transfer process involving adsorbed ions at solid/liquid interfaces by observing the effect of adsorbed ions to the electronic interactions and thermal energy transfer.

The principle and the experimental setup of the SPR-TRG is the same as described in our previous review, except for the arrangement for the optically exciting surface plasmons as shown in Fig. 9.²⁹ A mode-locked Q-switched Nd:YAG laser (Quantronix, model 416) was used as a light source, and the frequency was doubled using a nonlinear optical crystal. The pulse train wavelength was 532 nm with a repetition rate of 1 kHz and a pulse width of 80 ps in full width at half maximum. The pulse was separated into pump and probe pulses using partial reflective mirror. The pump beam was further divided into two beams by a half mirror. The two pump pulses were crossed and irradiated onto the same spot of the sample surface so as to coincide in time to form an interference pattern. The probe pulse was irradiated at the center of the spot after passing through a computer-controlled optical delay line. The reflecting diffracted light was monitored with a photomultiplier (PMT) connected to a flexible light guide, whose entrance was placed at one of the first order reflecting diffraction spots. The output signal from the PMT was gated and averaged over one millisecond with a boxcar integrator before an analog-to-digital transformation for computer storage. The spot diameters of the pump and probe beams were 60 and 40 μm , respectively.

The sample was a gold film (thickness 40 nm) vapor deposited on the surface of a hemicylindrical glass prism (LaSF15) with a refractive index of 1.89. The Kretschmann configuration was employed as the sample arrangement for the surface plasmon (SP) resonance (Fig. 9). Two pump pulses and one probe pulse were incident from the prism side onto the gold film. The sample was loaded on a rotary stage to allow the incident angle of the laser beams to be changed.

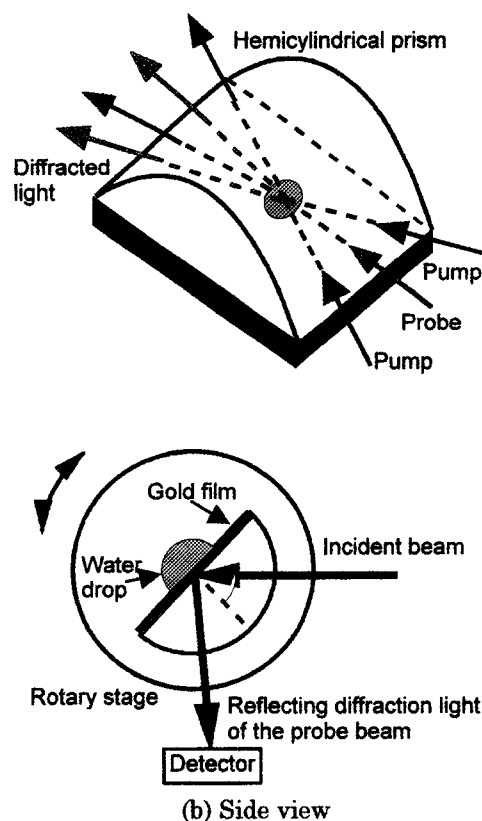


Fig. 9. Schematic illustrations of the arrangement of the sample and laser beams. The two pump beams overlapped and formed an interference fringe pattern on the gold film/prism interface. The generated transient grating was detected by the reflecting diffraction of the probe beam. The incident angle was kept to the surface plasmon angle, 54 degrees. The gold/solution interface was prepared using a drop of NaCl aqueous solution at the focused point.

The incident angle was fixed to the SP resonance angle, which was larger than the total reflectional angle. The SP was excited only by the p-polarized light, and was thus controlled by changing the polarization of the pump and the probe beams with two half-wave plates.

By applying both the pump and probe beams to the SP resonance condition, the relaxation signal of hot electrons within several picoseconds can be detected with 100 times larger intensity than the conventional TRG method.^{26,27} This decay signal is observed as a convoluted waveform with an incident pulse whose duration is 80 ps. On the other hand, when only the probe light is under the SPR condition, no signal for the hot electrons is detected. In this case, only the temperature rise after relaxation of the hot electrons and the following thermal diffusion are detected with 20-times larger intensity. In this study, we obtained information on electronic interaction involving hot electrons from the measurements in which both the pump and probe beams are under the SP resonance condition, and information on thermal diffusion across the interface from those in which only the probe light is under the SP resonance condition.

The Au/NaCl (aq) interfaces were prepared as shown in Fig. 9(b) using a drop of NaCl (aq) at the focusing point. The concentrations of NaCl (aq) were 0, 0.01, 0.1, 0.25, 0.5 M. As stated above, the experiments were carried out under two conditions: the SPR conditions for both the pump and probe beams, and for only the

probe beam. The spacing of the induced interference fringes was $2.14\ \mu\text{m}$ for all the measurements.

Figure 10 shows the TRG signals for the Au/water and Au/air interfaces. Figures 10(a) and 10(b) are the ones under the SP resonance conditions of both the pump and probe beams, and of only the probe beam, respectively. The signals were measured under the same conditions of laser intensity, detector sensitivity, and optics alignment. The waveforms in Fig. 10(a) include sharp peaks appearing at the same time as the pulse duration, followed by an exponential decay. The relaxation times of the exponential decay are 1 ns for the Au/air interface and over 5 ns for the Au/water interface. Some oscillations are also observed in the exponential decay for the Au/water interface. The difference in the waveforms of (a) and (b) is the peak at time zero.

The peak around time zero is due to the refractive index change by hot electrons induced by SP.^{26,27} The difference in the peak intensities between the Au/air interface and the Au/water interface is due to the difference in the signal enhancement factor for the SP resonance of each interface. The subsequent relaxations after the peak are due to thermal diffusion perpendicular to the interface. In

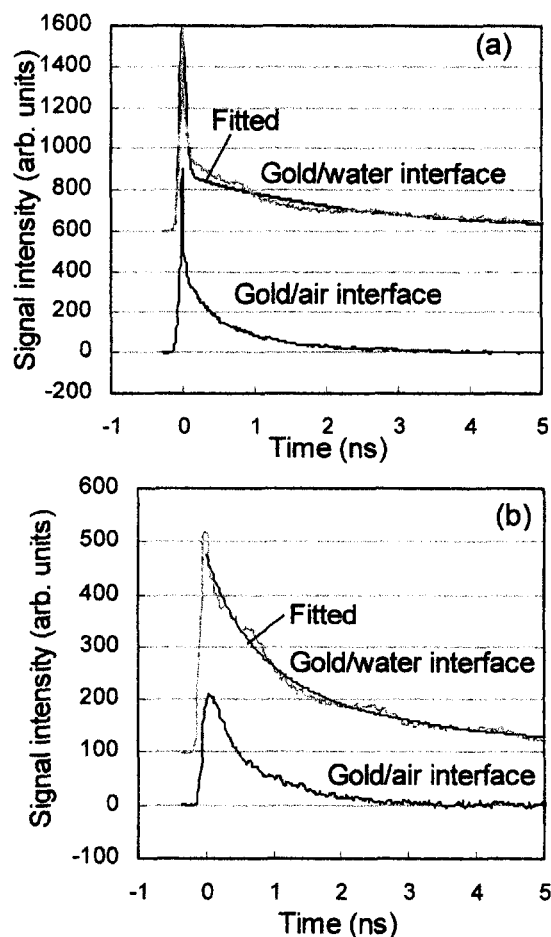


Fig. 10. Transient reflecting grating responses for the gold (40 nm)/air and gold (40 nm)/water interface when both the pump and probe beams were under the surface plasmon resonance condition (a) and when only the probe beam is under the surface plasmon resonance condition (b). In both (a) and (b), the waveforms for the gold/water interface are vertically displaced for clarity. The fitted curves were also shown for the signals at the gold/water interface.

Figs. 10(a) and 10(b), oscillations are observed in the relaxation curve. These were observed only for the solid/liquid interface, and they can be attributed to acoustic waves in the liquid phase near to the interface which were generated by the holographic thermal conduction from solid to liquid. It is estimated that the wave is localized approximately within 20 nm from the interface because the thermal diffusion length for 5 ns is 17 nm. In a word, the oscillations are due to the density change of the liquid phase close to the interface induced by an acoustic wave.

In order to examine the influence of the adsorbed ions to the energy transfer process at the solid/liquid interface, the TRG measurements were performed for Au/NaCl (aq) (0–0.5 M, $M = \text{mol dm}^{-3}$) interfaces under two kinds of SPR conditions as stated above. We intended to study the effect of chloride ions, which easily adsorb to the Au surface.^{31–33} The result showed a systematic change with increasing NaCl concentration.

Here we introduce two parameters: A_1 and A_2' . All the waveforms were fitted using exponential decay functions. A_1 is the intensity of the faster component due to the relaxation of hot electrons on a time scale of picosecond, and A_2' is for the slower component due to the thermal diffusion. The dependence of A_1 and A_2' on the NaCl concentration is shown in Fig. 11. With increasing the concentration, A_1 decreases and A_2' increases.

The physical meaning for the decrease of A_1 is difficult to clarify. However, it can be said the adsorbed ions have some influence on the electronic excitation and relaxation process. The increase in A_2' is due to the temperature rise in Au phase. The temperature rise originates in the heat generated by the relaxation of the hot electrons. This result shows that the heat generation increases with increasing the number of adsorbed ions. However, the heat generation should be the same because there is no absorption change of the sample under the same experimental condition. This discrepancy suggests that an ultrafast interfacial energy transfer takes place prior to the heat diffusion and that this transfer process is hindered by the adsorbed ions. Our assumption is that hindrance of the ultrafast interfacial energy transfer by the adsorbed ions results

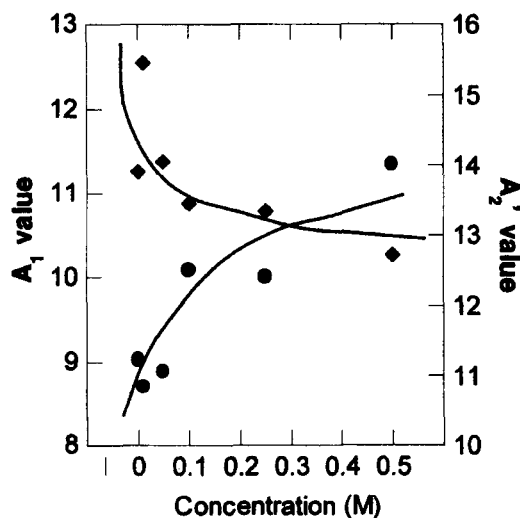


Fig. 11. The dependence of the A_1 (◆) and A_2' (●) values on the NaCl concentration. The tendencies of A_1 and A_2' are shown with smooth lines. A_1 and A_2' are fitting parameters for the transient reflecting grating signals with SPR of both pump and probe beams and only the probe beam respectively. The detailed meanings are explained in the Section 2.

in the decrease of the interaction between the hot electrons and adsorbed ions (corresponding to the decrease in A_1), and the increase of heat generation (corresponding to the increase in A_1). In a word, there are ultrafast energy transfer processes from the hot electrons to water molecules, competing with the heat generation of gold. These results reflect interfacial fundamental processes on a molecular scale. We assume that the initial energy transfer is caused by an interaction between the polarization and the dipole moment of the water molecules, and that the initial energy transfer is hindered by the screening of the transient polarization by the oriented interfacial water molecules.

4. Conclusions

Ultrafast dynamics at solid/liquid interfaces was investigated using our developed photothermal techniques: femtosecond transient reflectivity (fs-TR) method, femtosecond transient reflecting grating (fs-TRG) method, and picosecond surface plasmon resonance transient reflecting grating (ps-SPR-TRG) method. Firstly, Pt/aqueous electrolyte interfaces were measured using the fs-TR method. A novel ultrafast relaxation component (20 fs) was found in the Pt/HCl (aq) and Pt/H₂SO₄ (aq) interfaces, in which the anions (Cl⁻ and SO₄²⁻) have strong affinity to the Pt surface. It was suggested that this is due to the scattering of non-thermalized electrons by adsorbed anions. Secondly, TiO₂/KSCN (aq) interfaces were measured using the fs-TRG method. Ultrafast relaxation components (110–690 fs) were observed for the first time in the TRG signals. This indicates ultrafast transfer of nonequilibrium holes occurs and should be taken into account in interfacial reaction. Thirdly, Au/NaCl (aq) interfaces were measured using ps-SPR-TRG method, focusing at both the behavior of hot electrons and thermal diffusion. The result indicates that there is an ultrafast energy transfer process, which is affected by adsorbed ions.

In this review, we presented unambiguous evidence of ultrafast energy transfer process involving hot electrons or holes at solid/liquid interfaces. Extension of the methodology to the femtosecond time region allowed the observation of ultrafast energy transfer by hot carriers. In particular, the fs-TRG method achieved the observation of interfacial ultrafast energy transfer with high S/N ratio. This owes to the principle of the TRG method and to the fabrication of the sample cell. Furthermore, by combining the picosecond TRG method with the SPR condition, the information on both electronic interaction and thermal energy transfer was obtained. Although its time resolution is on the order of picosecond, this method has advantages in the measurements of whole energy transfer process on an extensive time scale from picosecond to nanosecond. We believe this kind of work using ultrafast photothermal spectroscopy will contribute significantly to the knowledge of interfacial physical chemistry. Recently, we have developed a multi-wave femtosecond TRG method using a white light as a probe beam and a variable light as a pump beam.³⁴ This multi-wave TRG method will allow us to obtain more detailed information on ultrafast dynamics involving hot carriers.

This work was supported by Grants-in-Aid for Specially Promoted Research (No. 07102004) and for Scientific Research on Priority Area of Electrochemistry of Ordered Interfaces (No. 09237219) from the Ministry of Education, Science, Sports and Culture.

References

- 1 H. Tributsch and L. Pohlmann, *Science*, **279**, 1891 (1998).
- 2 A. J. Nozik and R. Memming, *J. Phys. Chem.*, **100**, 13061 (1996).
- 3 A. L. Linsebigler, G. Lu, and J. T. Yates, *Chem. Rev.*, **95**, 735 (1995).
- 4 M. A. Fox and M. T. Dulay, *Chem. Rev.*, **93**, 34 (1993).
- 5 N. Serpone and E. Pelizzetti, "Photocatalysis," Wiley, New York (1989).
- 6 J. M. Lantz and R. M. Corn, *J. Phys. Chem.*, **98**, 4899 (1994).
- 7 C. S. Turchi and D. F. Ollis, *J. Catal.*, **119**, 483 (1989).
- 8 D. Bicanic, "Photoacoustic and Photothermal Phenomena," Springer-Verlag, Berlin (1992).
- 9 S. Deliwala, R. J. Finlay, J. R. Goldman, T. H. Her, W. D. Mieher, and E. Mazur, *Chem. Phys. Lett.*, **242**, 614 (1995).
- 10 S. Gao, D. G. Busch, and W. Ho, *Surface Sci.*, **344**, L1252 (1995).
- 11 W. S. Fann, R. Storz, H. W. K. Tom, and J. Bokor, *Phys. Rev. Lett.*, **68**, 2834 (1996).
- 12 T. Hertel, E. Knoesel, M. Wolf, and G. Ertl, *Phys. Rev. Lett.*, **76**, 535 (1996).
- 13 M. E. Schmidt and P. Guyot-Sionnest, *J. Chem. Phys.*, **104**, 2438 (1996).
- 14 A. Harata and T. Sawada, *Trends Anal. Chem.*, **14**, 504 (1995).
- 15 A. Harata, "Proc. Int. Seminar on Photothermal Phenomena and Their Applications," Tomakomai, Japan, Abstr., p. 64 (1998).
- 16 A. Hibara, A. Harata, and T. Sawada, *Chem. Phys. Lett.*, **272**, 1 (1997).
- 17 Q. Shen, A. Harata, and T. Sawada, *Jpn. J. Appl. Phys.*, **32**, 3628 (1993).
- 18 H. Nishimura, A. Harata, and T. Sawada, *Jpn. J. Appl. Phys.*, **32**, 5149 (1993).
- 19 A. Hibara, T. Morishita, I. Tsuyumoto, A. Harata, and T. Sawada, "Proc. Int. Seminar on Photothermal Phenomena and Their Applications," Tomakomai, Japan, Abstr., p. 209 (1998).
- 20 T. Morishita, A. Hibara, I. Tsuyumoto, A. Harata, and T. Sawada, "Proc. Int. Seminar on Photothermal Phenomena and Their Applications," Tomakomai, Japan, Abstr., p. 219 (1998).
- 21 A. Harata, T. Kawasaki, M. Ito, and T. Sawada, *Anal. Chim. Acta*, **299**, 349 (1995).
- 22 A. Harata, Q. Shen, and T. Sawada, *Physica B*, **219**, 629 (1996).
- 23 A. Harata, T. Edo, and T. Sawada, *Chem. Phys. Lett.*, **249**, 112 (1996).
- 24 T. Morishita, A. Hibara, T. Sawada, and I. Tsuyumoto, *J. Phys. Chem. B*, **103**, 5984 (1999).
- 25 K. Katayama, Q. Shen, A. Harata, and T. Sawada, *Appl. Phys. Lett.*, **69**, 2468 (1996).
- 26 K. Katayama, Q. Shen, A. Harata, and T. Sawada, *Phys. Rev. B*, **58**, 8428 (1998).
- 27 K. Katayama, I. Tsuyumoto, A. Harata, and T. Sawada, *Bull. Chem. Soc. Jpn.*, **72**, 2383 (1999).
- 28 K. Katayama, I. Tsuyumoto, A. Harata, and T. Sawada,

"Proc. Int. Seminar on Photothermal Phenomena and Their Applications," Tomakomai, Japan, Abstr., p. 213 (1998).

29 A. Harata, Q. Shen, and T. Sawada, *Ann. Rev. Phys. Chem.*, **50**, 193 (1999).

30 S. D. Brorson, J. G. Fujimoto, and E. P. Ippen, *Phys. Rev. Lett.*, **59**, 1962 (1987).

31 Z. Shi, S. Wu, and J. Lipkowski, *J. Electroanal. Chem.*, **384**,

171 (1995).

32 Z. Shi and J. Lipkowski, *J. Electroanal. Chem.*, **403**, 225 (1996).

33 A. Kolics, A. E. Thomas, and A. Wieckowski, *J. Chem. Soc., Faraday Trans.*, **92**, 3727 (1996).

34 K. Katayama, Y. Inagaki, and T. Sawada, *Phys. Rev. B*, in press.



Isao Tsuyumoto was born in 1969 in Hyogo Prefecture, Japan. He received his B. Eng. degree in 1991, M. Eng. degree in 1993, and Ph. D. degree in 1996, all from the University of Tokyo, Japan. He was a research associate of the Department of Applied Chemistry, School of Engineering, the University of Tokyo from 1996 to 1999. He was engaged in laser spectroscopy at solid/liquid and liquid/liquid interfaces, and physical chemistry in heterogeneous systems. Now he is an assistant professor at the Department of Environmental Systems Engineering, Kanazawa Institute of Technology. His current interests include application of laser spectroscopy to heterogeneous systems, and characterization of inorganic materials using new methodologies.



Tsuguo Sawada was born in 1941 in Mie Prefecture, Japan. He received his B. of Engineering degree in 1965, his M. of Engineering degree in 1967, and his Ph.D in 1970 from the University of Tokyo. He is now Professor of Department of Advanced Materials Sciences at the University of Tokyo.

Dr. Sawada's research interests include photoacoustic and photothermal spectroscopies, laser applied spectroscopy, development of new methodology, and material evaluation using optical methods. Recently, he feels particular interest in applying these above-mentioned laser spectroscopies to evaluation of liquid/liquid and solid/liquid interfaces.

For the above academic activities, the Japan Society of Analytical Chemistry awarded him a prize in 1995. Several other prizes have also been received.